

209

~~CONFIDENTIAL~~

Copy
RM L54H09

NACA RM L54H09

ESS410



TECH LIBRARY KAFB, NM

NACA

RESEARCH MEMORANDUM

DRAG MEASUREMENTS ON A 1/6-SCALE, FINLESS, STING-MOUNTED
NACA RM-10 MISSILE IN FLIGHT AT MACH NUMBERS FROM
1.1 TO 4.04 SHOWING SOME REYNOLDS NUMBER
AND HEATING EFFECTS

By Robert O. Piland

Langley Aeronautical Laboratory
Langley Field, Va.

CLASSIFIED DOCUMENT

~~Special sensitive information~~
NATIONAL ADVISORY COMMITTEE
FOR AERONAUTICS

WASHINGTON

October 27, 1954

~~CONFIDENTIAL~~

REF ID: A65211

By / Uth

B,

11:20 (Unclassified.....)
Asst. Tech. R. W. H. (Unclassified # 33
(ORANGE)

24 Aug 55.....

WV

~~GRADE~~ U.S. AIR FORCE
U. S. AIR FORCE

1H

NACA RM L54H09



NATIONAL ADVISORY COMMITTEE FOR AERONAUTICS

RESEARCH MEMORANDUM

DRAG MEASUREMENTS ON A 1/6-SCALE, FINLESS, STING-MOUNTED

NACA RM-10 MISSILE IN FLIGHT AT MACH NUMBERS FROM

1.1 TO 4.04 SHOWING SOME REYNOLDS NUMBER

AND HEATING EFFECTS

By Robert O. Piland

SUMMARY

A 1/6-scale, finless NACA RM-10 missile sting-mounted on a parent body has been flight tested to a peak Mach number of 4.04. Measurements of total drag, base drag, and wall temperature were obtained. Reynolds numbers of 17×10^6 to 47×10^6 , based on body length, corresponding to Mach numbers 1.07 to 4.04 were encountered.

The total- and base-drag measurements correlated well with wind-tunnel results at Mach numbers between 1.5 and 2.0 and at a Mach number of 4. Measured base pressure coefficients were also seen to agree excellently with calculations made by using Love's method (NACA RM L53C02).

The friction drag of the model was estimated by using a calculated pressure drag in combination with the measured total and base drag. This estimate in conjunction with a consideration of the Reynolds number and heating conditions during the flight indicate the existence of considerable regions of laminar flow on the body throughout the flight.

INTRODUCTION

The performance of high-speed, long-range missiles is dependent upon the friction drag because it is such a large part of the total drag. Consequently, experimental data showing effects of Mach number, Reynolds number, and aerodynamic heating on body drag are valuable to the missile designer either for direct use or to evaluate available theoretical approaches.

As part of a program (refs. 1 to 4) to provide such data, a 1/6-scale NACA RM-10 missile sting-mounted on a parent body has been flown. The model reached a maximum Mach number of 4.04. Total drag, measured by means of a drag balance, base drag, and skin temperature were obtained. These data in conjunction with estimates of forebody pressure drag made an assessment of the friction drag possible.

In addition, because the Reynolds numbers of the test were lower than the usual flight test Reynolds numbers, correlation of total and base drag with previous wind-tunnel investigations is possible. Such a correlation was lacking in the summary of the data for the NACA RM-10 missile of reference 5. The Reynolds numbers range of the test, corresponding to Mach numbers of 1.07 and 4.04, is 17×10^6 and 47×10^6 , respectively. Reynolds numbers are based on total body length. The test was conducted at the Langley Pilotless Aircraft Research Station at Wallops Island, Va.

SYMBOLS

t	time, sec
M	Mach number
T _w	skin temperature, °R
T ₀	free-stream static temperature, °R
R	Reynolds number, based on body length
T _{AW}	adiabatic wall temperature, °R
$C_D = \frac{\text{Drag}}{qS}$	
q	dynamic pressure, lb/sq ft
S	model frontal area, 0.0214 sq ft
$\frac{\Delta P}{q} = \frac{P_b - P_0}{q}$	
P _b	base pressure, lb/sq ft
P ₀	free-stream static pressure, lb/sq ft

NACA RM 154H09

3

Subscripts:

T total
B base
P forebody pressure
f friction

MODELS AND TESTS

A sketch of the test vehicle consisting of a 1/6-scale, finless NACA RM-10 missile sting-mounted on a parent body is shown in figure 1. Figure 2(a) presents a more detailed sketch of the NACA RM-10 missile. Figure 2(b) presents a photograph of the model. The dull finish is due to a protective plastic coating which was removed before testing; actually, the model was highly polished. The model was constructed from 0.032-inch-thick Inconel skin which had a break at station 15 to allow installation of a resistance-type temperature pickup, described in reference 6. The pickup was located at station 11.2. Orifices for the measurement of base pressure were located on the model sting just forward of the base of the model (see fig. 2). The total drag of the NACA RM-10 missile was obtained by use of a drag balance contained in the parent body. The telemeter and other instrumentation which relayed the measurements of drag, base pressure, and skin temperature to a ground receiving station were also contained in the parent body. The long cylindrical section of the parent body consisted of a 6.25-inch ABL Deacon rocket motor. Stabilizing fins were attached to the rear end of the rocket motor.

A photograph of the test vehicle and booster on the launcher is shown in figure 3. The booster, consisting of two 6.25-inch ABL Deacon rocket motors and stabilizing fins, accelerated the model to a Mach number of approximately 1.7. The sustainer, ignited immediately thereafter, further accelerated the model to its peak Mach number of 4.04. The model was tracked by CW Doppler velocimeter which afforded velocity data, and by SCR 584 radar unit, which gave the model trajectory. Radiosonde data provided the variation of static pressure and temperature with altitude.

Figure 4 presents the variation of Mach number, Reynolds number, and temperature ratio T_w/T_o with time. Figure 5 presents the variation of wall temperature with flight time. Figure 6 presents the variation of Reynolds number and temperature ratio T_w/T_o with Mach number.

ACCURACY OF MEASUREMENTS

The accuracy of the test measurements is estimated to be within the following limits. (The accuracy of the Mach number was ± 0.005 .)

Measurement	Accuracy of measurement for Mach numbers of -				
	1.2	1.6	2.0	3.0	4.0
C_{DT}	± 0.020	± 0.013	± 0.008	± 0.004	± 0.003
C_{DB}	$\pm .008$	$\pm .004$	$\pm .003$	$\pm .001$	$\pm .001$
$\frac{P_b - P_o}{q}$	$\pm .022$	$\pm .011$.008	$\pm .003$	$\pm .003$

RESULTS AND DISCUSSION

Total Drag

The total- and base-drag coefficients, based on maximum body frontal area, are presented in figure 7 for Mach numbers between 1.07 and 4.04. The Reynolds number and heating conditions corresponding to these Mach numbers are shown in figure 6. Wind-tunnel measurements from the Langley 4- by 4-foot supersonic pressure tunnel, the Langley 9- by 9-inch Mach number 4 blowdown jet, and the Lewis 8- by 6-foot supersonic tunnel are also presented in figure 7. These measurements have been corrected theoretically to flight heating and Reynolds number conditions by using reference 7 and assuming equilibrium heating conditions for the tunnel models. The corrections were on the order of 5 percent. Agreement within 10 percent is seen to exist between the flight and the corrected wind-tunnel data. The flight results in all cases were slightly lower than the wind-tunnel results.

In order to evaluate these measurements to show better the individual effects of Mach number, Reynolds number, and heating, the total drag is broken down into base drag (measured), pressure drag (calculated), and friction drag ($C_{DF} = C_{DT} - C_{DB} - C_{DP}$), and each drag is discussed separately.

CONFIDENTIAL

Base Drag

The base drag coefficients are presented in figure 7 and are compared with several wind-tunnel measurements. Reference 8 presents a method to predict the base pressures on an NACA RM-10 missile between Mach numbers 1 and 4. Comparison was made with wind-tunnel measurements between Mach numbers of 1.4 and 2.4 and it was concluded that the theories were adequate. In order to extend the Mach number range of experimental and theoretical correlation, the calculations of reference 8 are reproduced in figure 8 and compared with present flight measurements. Two calculated curves from reference 8 are shown, both of which were obtained by using the same method, the difference being that in one case the theory of Jones and Margolis was used to determine the Mach number at the trailing edge of the body and in the other case the theory of Lighthill was used. At Mach numbers from 4 to 1.4, the agreement is excellent. Below a Mach number of 1.4, the quantitative agreement became poorer but the predicted trend is still evident in the measured data. The poor agreement in this Mach number range is possibly due to the reduced accuracy of the test.

Pressure Drag

The method of characteristics (ref. 9) was used to calculate the pressure drag of the body. These calculations are presented in figure 9 where they are compared with wind-tunnel measurements at several Mach numbers. The comparison indicates to some extent the accuracy of the theory which will be used to obtain the friction drag of the model.

Friction Drag

The friction drag of the model was determined by subtracting the calculated pressure drag (fig. 9) and measured base drag from the measured total drag. Values of friction drag, varying with time, are presented in figure 10. The variation with time is presented because the three affecting parameters, namely, Mach number, Reynolds number, and thermal ratio, vary considerably during the flight, and thus variation of the drag with any one of these parameters would be meaningless. Figure 10 also presents the variation of the three parameters mentioned above.

The friction drag of the model as predicted by the theory of reference 7 is compared with the measured drag in figure 10. The theory, which assumes the model boundary layer to be turbulent, is seen to predict drag values which are higher than those measured. The most obvious explanation of this difference lies in the probability of regions of laminar flow existing on the model during the test.

When the data are considered in detail, the drag is seen to rise during the early portion of the flight and reaches a maximum at about 2.8 seconds. It is believed that, during this time, the transition Reynolds number is decreasing slightly because of the increasing Mach number in the absence of any considerable cooling of the boundary layer. The degree of cooling can be seen in figure 10, indicated by the difference in wall temperature (T_w/T_o) and adiabatic wall temperature (T_{aw}/T_o). This difference is seen to increase through the test range and reaches a maximum at a Mach number of 4. The friction drag is seen to decrease above 2.8 seconds, and the percentage difference between theory and experiment increases for the remainder of the time for which data are presented. If the theory is assumed to be correct for a completely turbulent boundary layer, this increasing percentage difference between theory and experiment would indicate an increasing Reynolds number of transition. At maximum Mach number ($t = 7.4$ seconds), a Reynolds number of transition of about 24×10^6 would be necessary to account for the difference in theory and experiment. Attaining this Reynolds number of transition may be possible when the effect of cooling on transition is considered. For example, data in reference 10 for an RM-10 missile, shows a Reynolds number of transition of 28×10^6 to be obtainable with less cooling than is encountered in the present test.

In addition to the boundary layer being cooled during the test, it is interesting to note that the temperature condition of the model is in a region which would promote stability of the laminar boundary layer (ref. 11) and theoretically allow an infinite length of laminar boundary layer. This region is shown in figure 10. The measured drag values are of such magnitude as to preclude the existence of laminar flow over the whole body but partial coverage seems likely. This condition (infinite stability) exists on the model between 2.7 and 6.5 seconds.

CONCLUSIONS

A sting-mounted, finless, 1/6-scale NACA RM-10 missile has been flight tested and total-drag, base-pressure, and wall-temperature measurements have been obtained between Mach numbers of 1.07 and 4.04 corresponding to Reynolds numbers based on body length of 17×10^6 and 47×10^6 . The following observations were made from the data when correlated with wind-tunnel results and theory.

1. Good agreement is attained between wind-tunnel and flight measurements of total and base drag between Mach numbers of 1.5 and 2.0 for similar Reynolds number conditions.

NACA RM L54H09

7

2. The method of Love (NACA RM L53C02) utilizing the theory of either Jones or Lighthill is shown to be excellent for the prediction of base pressures on the NACA RM-10 body at Mach numbers from 1.4 to 4.

3. A consideration of the Reynolds numbers and heating conditions on the model in conjunction with the derived friction drag indicates the existence of considerable regions of laminar flow on the body throughout the flight.

Langley Aeronautical Laboratory,
National Advisory Committee for Aeronautics,
Langley Field, Va., July 23, 1954.

REFERRENCES

1. Chauvin, Leo T., and deMoraes, Carlos A.: Correlation of Supersonic Convective Heat-Transfer Coefficients From Measurements of the Skin Temperature of a Parabolic Body of Revolution (NACA RM-10). NACA RM L51A18, 1951.
2. Rumsey, Charles B., and Loposer, J. Dan: Average Skin-Friction Coefficients From Boundary-Layer Measurements in Flight on a Parabolic Body of Revolution (NACA RM-10) at Supersonic Speeds and at Large Reynolds Numbers. NACA RM L51B12, 1951.
3. Loposer, J. Dan: Average Skin-Friction Coefficients From Boundary-Layer Measurements on an Ogive-Cylinder Body in Flight at Supersonic Speeds. NACA RM L52K28a, 1953.
4. Chauvin, Leo T., and Maloney, Joseph P.: Experimental Convective Heat Transfer to a 4-Inch and 6-Inch Hemisphere at Mach Numbers From 1.62 to 3.04. NACA RM L53L08a, 1954.
5. Evans, Albert J.: The Zero-Lift Drag of a Slender Body of Revolution (NACA RM-10 Research Model) As Determined From Tests in Several Wind Tunnels and in Flight at Supersonic Speeds. NACA TN 2944, 1953.
6. Fricke, Clifford L., and Smith, Francis B.: Skin-Temperature Telemeter for Determining Boundary-Layer Heat-Transfer Coefficients. NACA RM L50J17, 1951.
7. Van Driest, E. R.: The Turbulent Boundary Layer for Compressible Fluids on a Flat Plate With Heat Transfer. Rep. No. AL-997, North American Aviation, Inc., Jan. 27, 1950.
8. Love, Eugene S.: The Base Pressure at Supersonic Speeds on Two-Dimensional Airfoils and Bodies of Revolution (With and Without Fins) Having Turbulent Boundary Layers. NACA RM L53C02, 1953.
9. Ferri, Antonio: Elements of Aerodynamics of Supersonic Flows. The MacMillan Co., 1949.
10. Czarnecki, K. R., and Sinclair, Archibald R.: Preliminary Investigation of the Effects of Heat Transfer on Boundary-Layer Transition on a Parabolic Body of Revolution (NACA RM-10) at a Mach Number of 1.61. NACA TN 3165, 1954. (Supersedes NACA RM L52E29a.)

2H

NACA RM 154H09

9

11. Van Driest, E. R.: Calculation of the Stability of the Laminar Boundary Layer in a Compressible Fluid on a Flat Plate With Heat Transfer. Rep. No. AL-1334, North American Aviation, Inc., Sept. 3, 1951. (Rev. Feb. 14, 1952.)

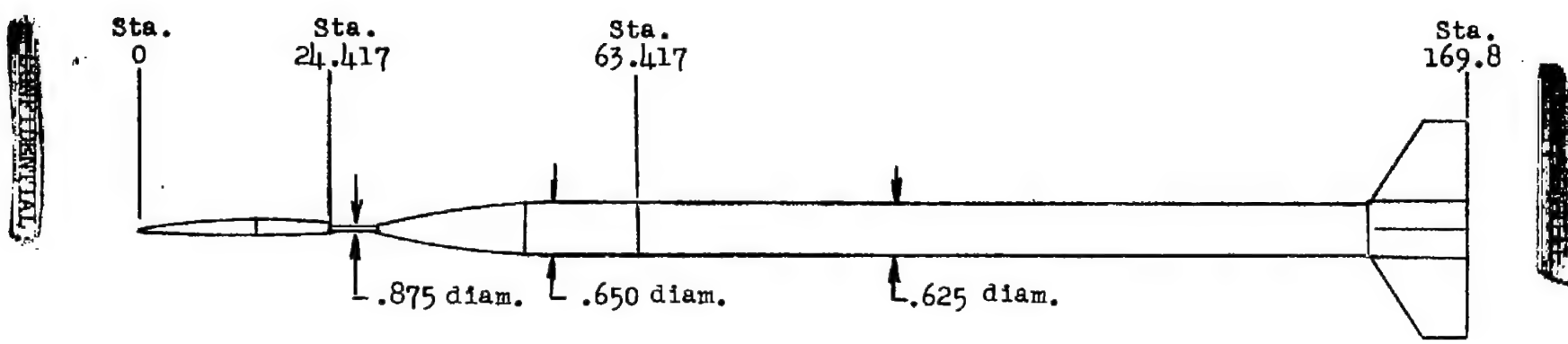
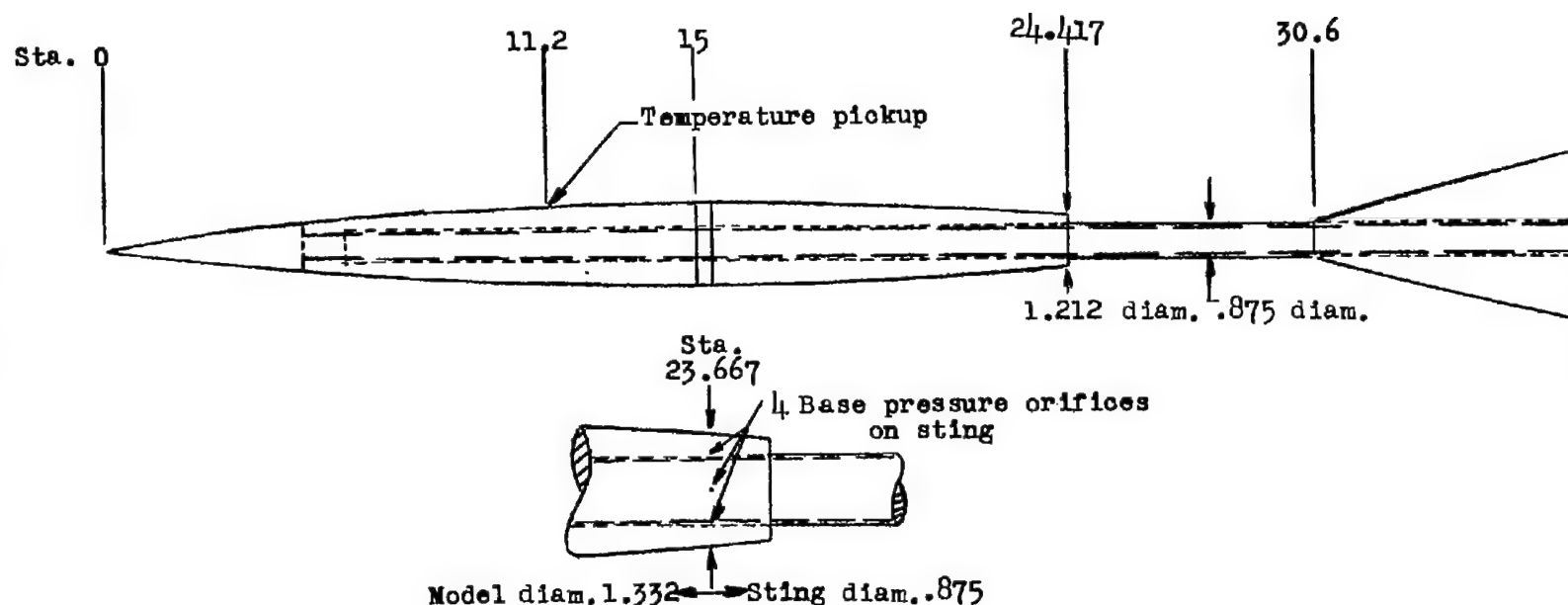


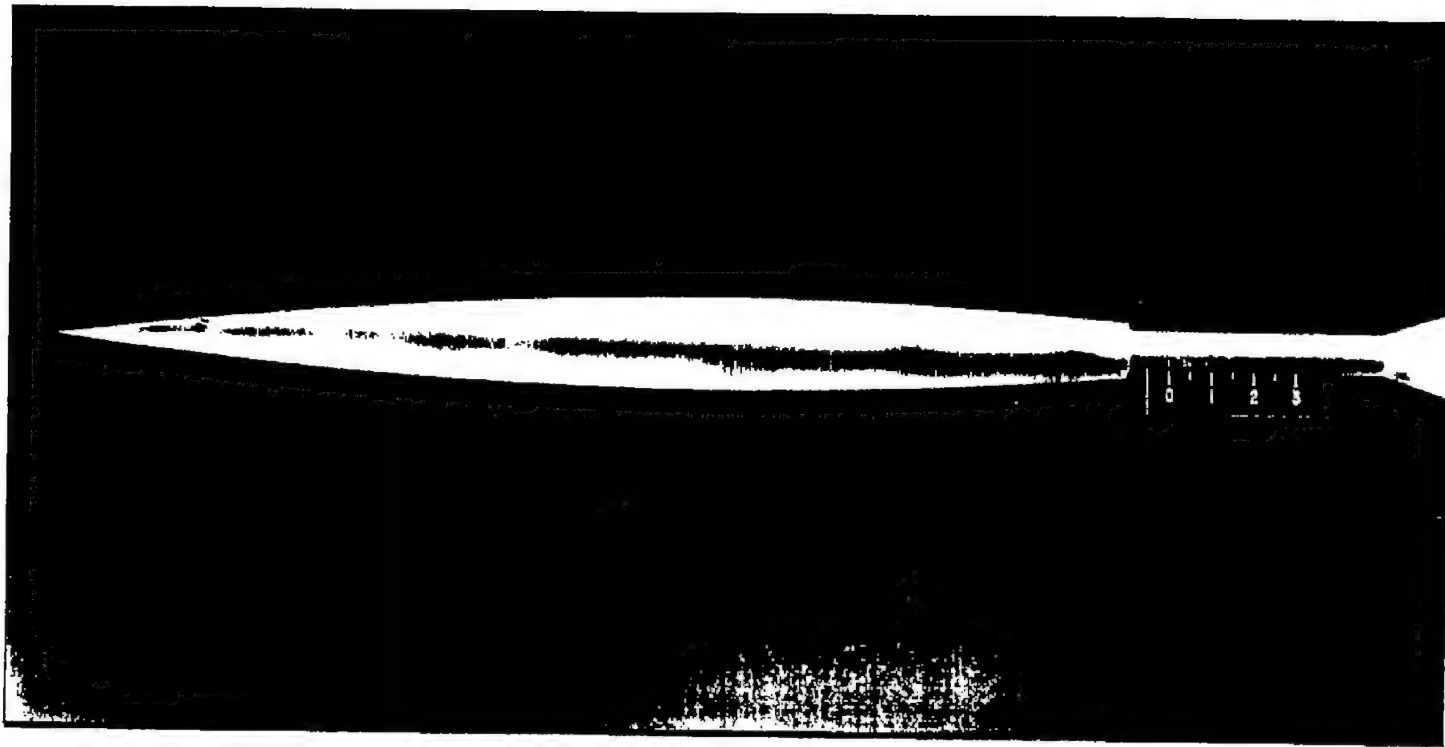
Figure 1.- Sketch of NACA RM-10 test model mounted on carrier body. All dimensions are in inches.

NACA RM 154H09



(a) Sketch of model. All dimensions are in inches.

Figure 2-- NACA RM-10 test vehicle.



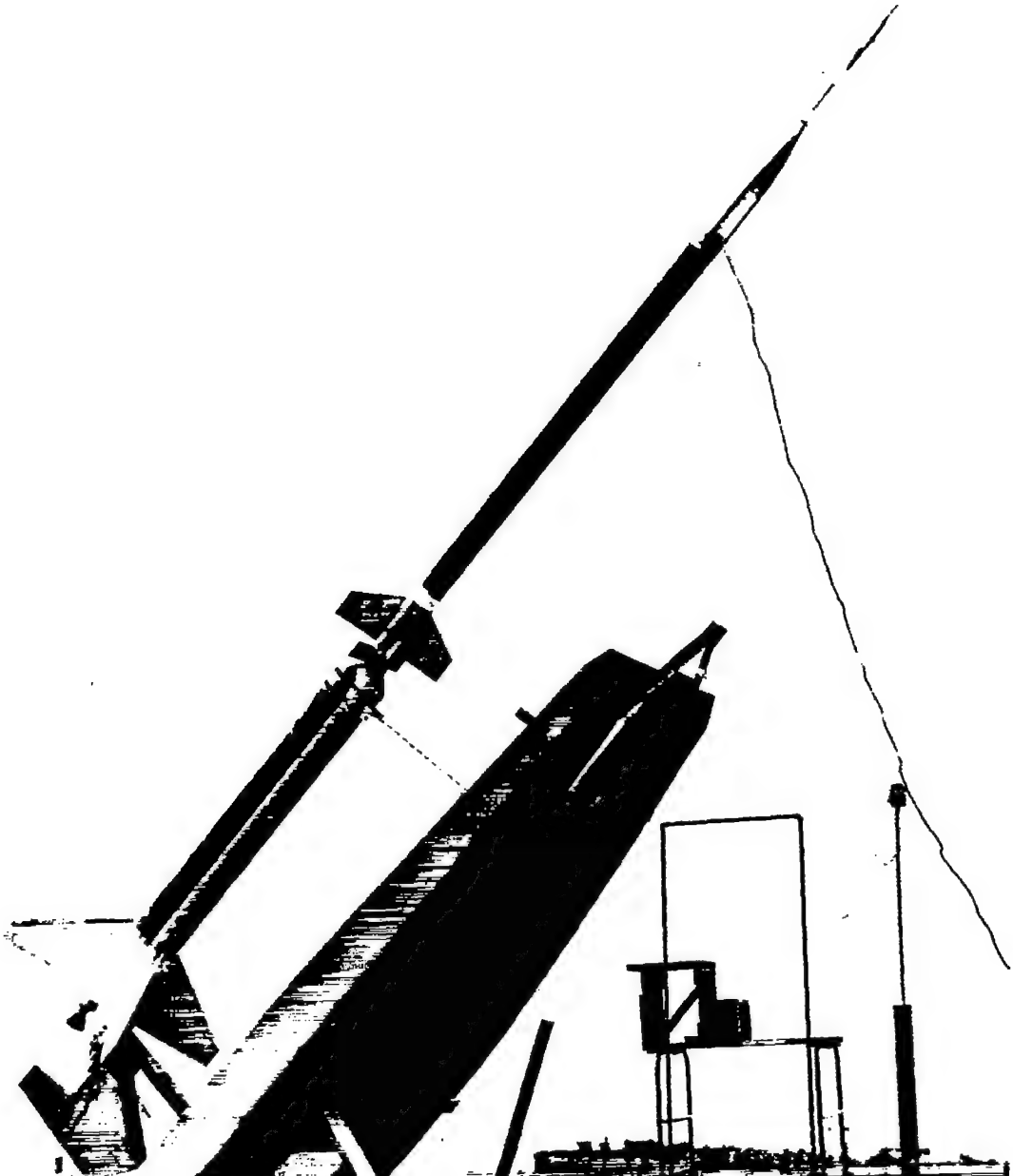
(b) Photograph of model.

L-71306

Figure 2.- Concluded.

NACA RM L54H09

13



L-73745

Figure 3.- Photograph of test vehicle on launcher.

14

NACA RM L54H09

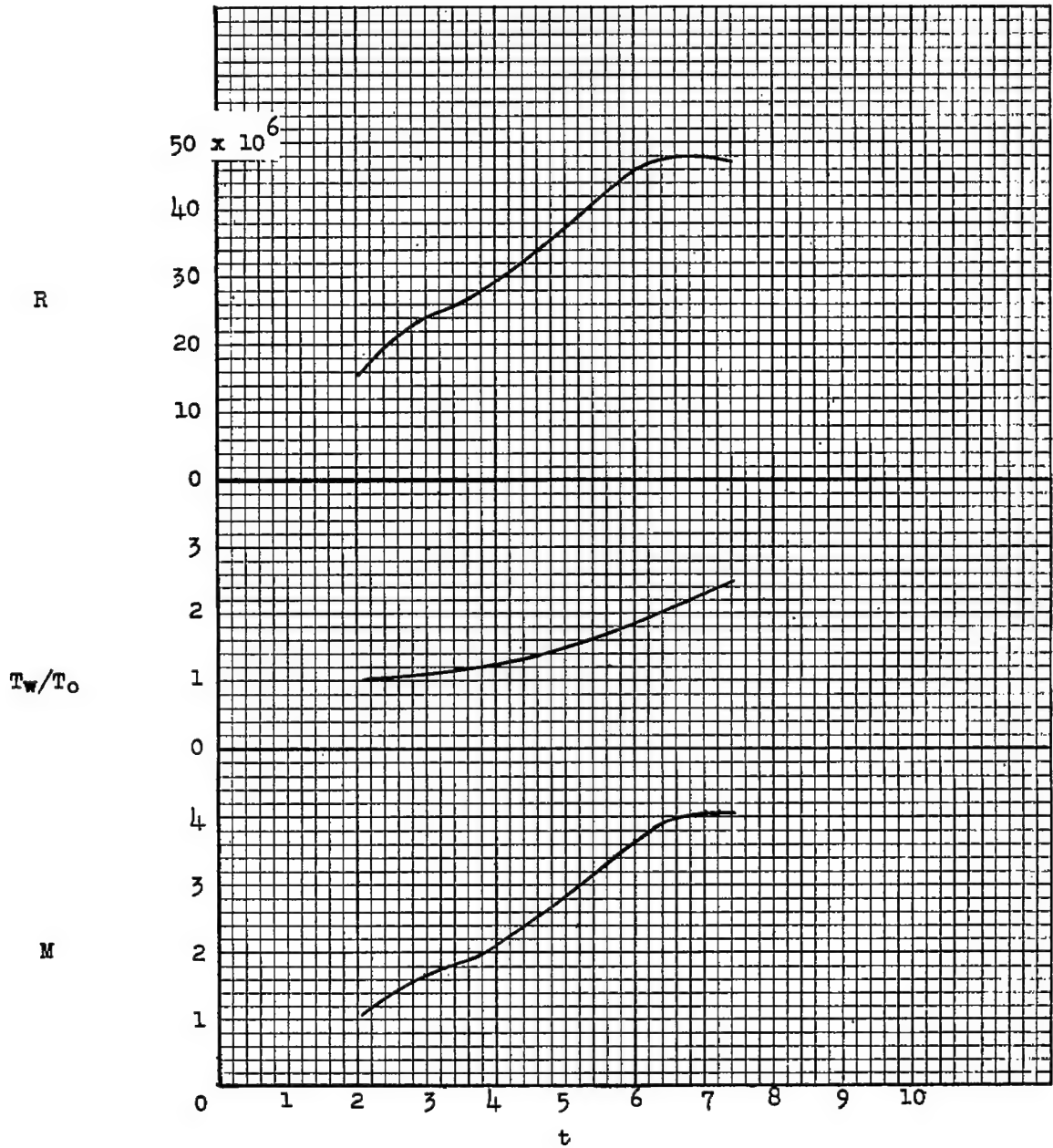


Figure 4.- Flight test conditions. Reynolds number based on body length.

CONFIDENTIAL

NACA RM L54H09

15

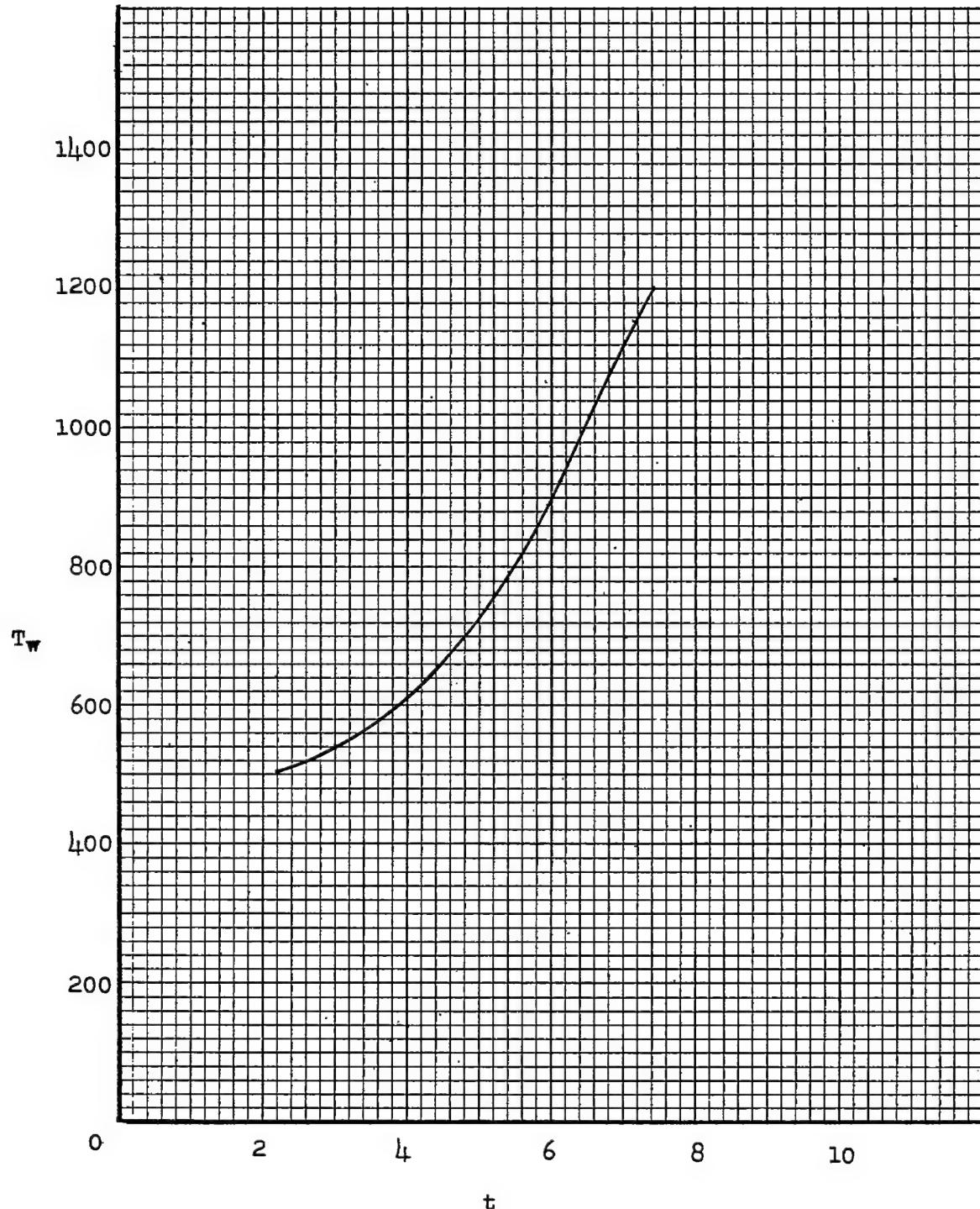


Figure 5.- Wall temperature at station 11.2 during flight.

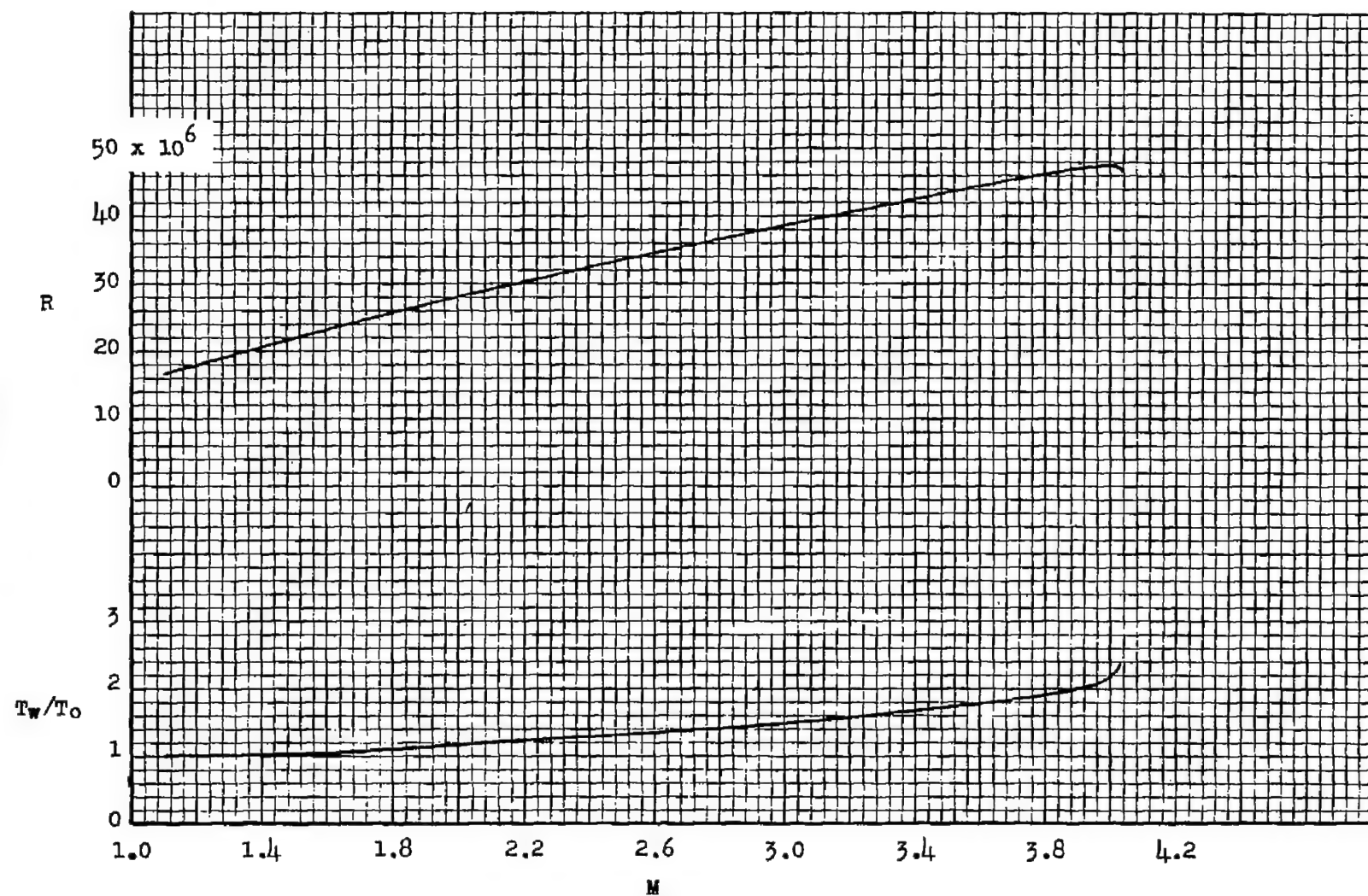


Figure 6.- Variation of Reynolds number, based on body length, and T_w/T_0 with Mach number.

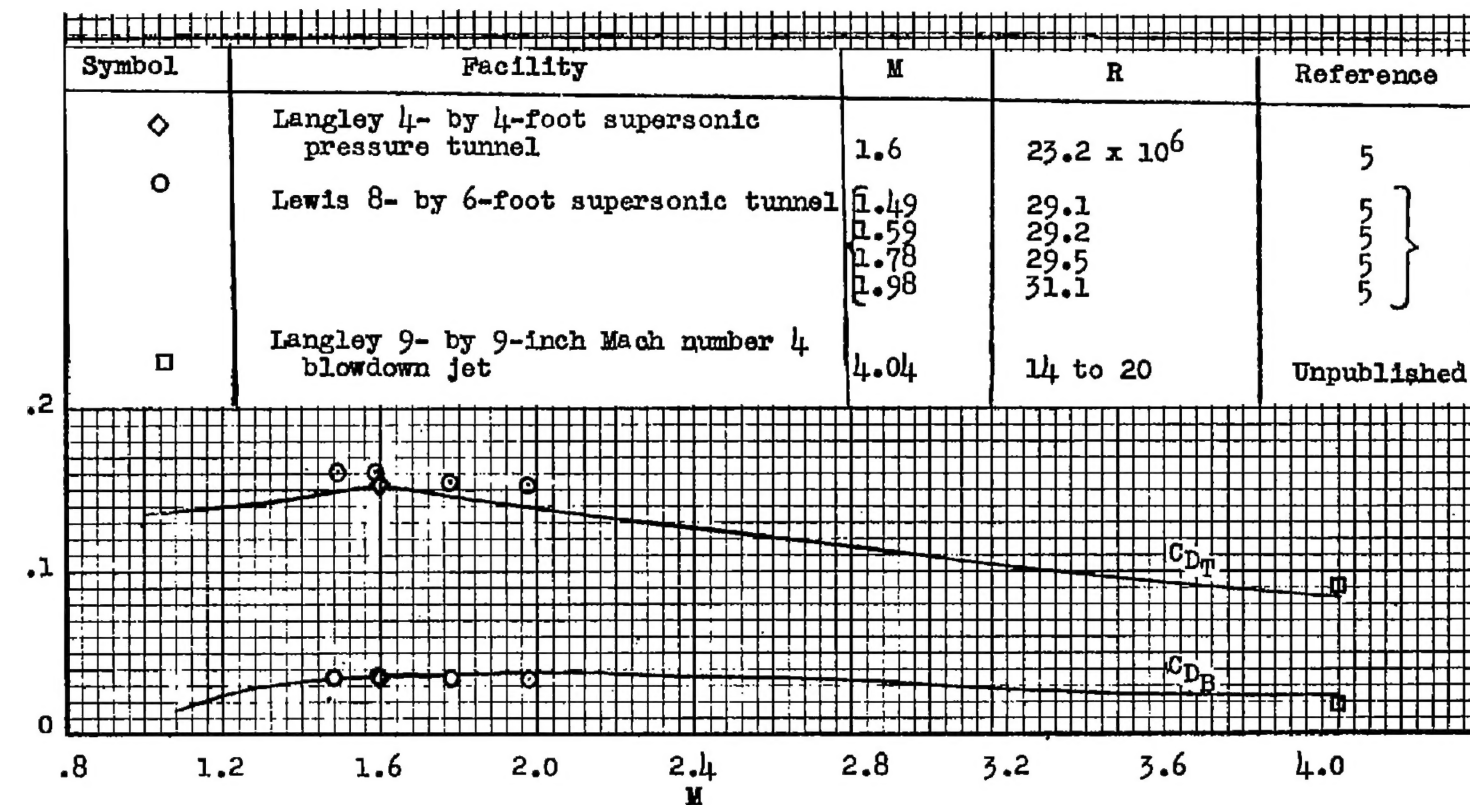


Figure 7.- Comparison of flight-test data with wind-tunnel results.

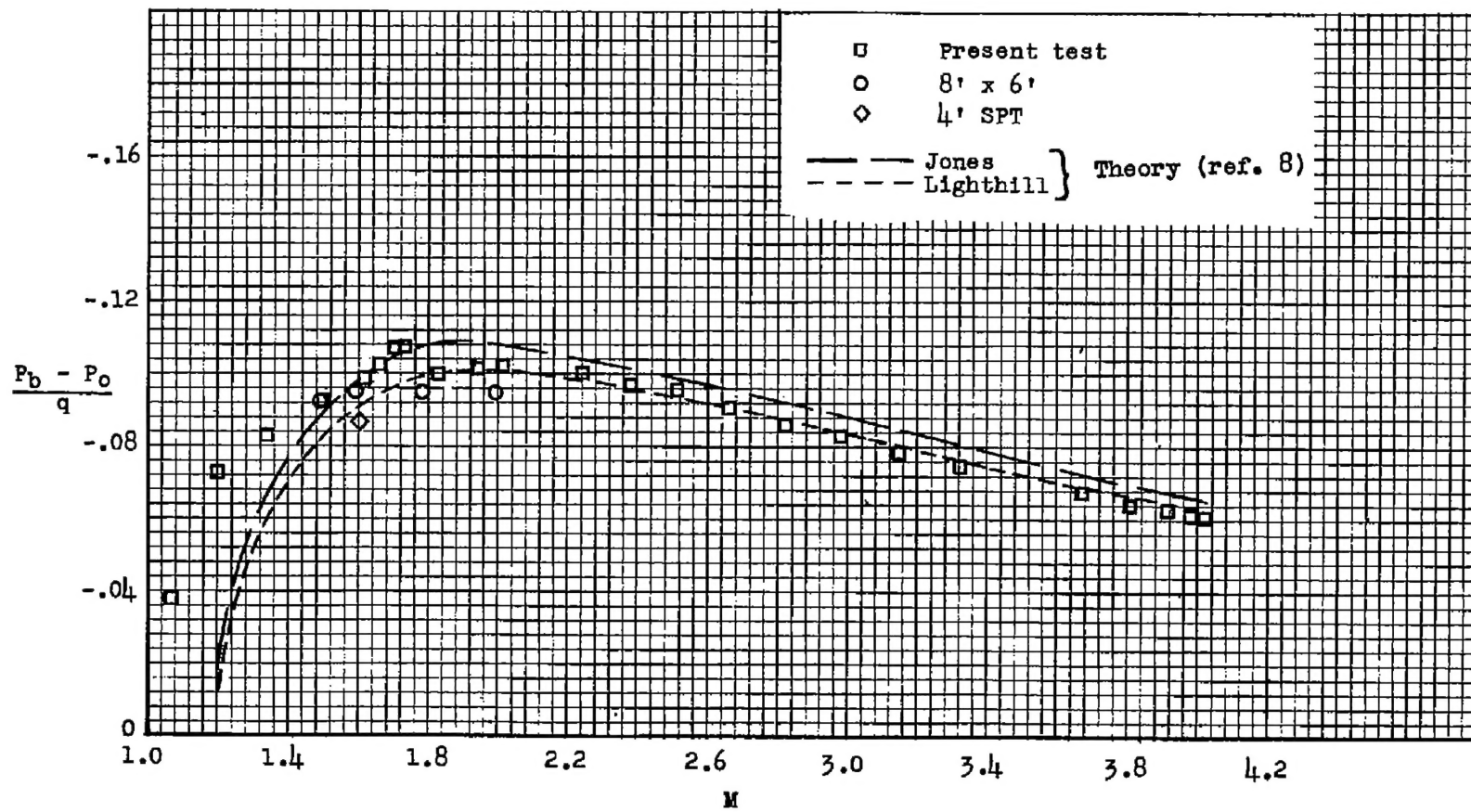


Figure 8.- Comparison of flight base-pressure coefficients with theory and other experimental data.

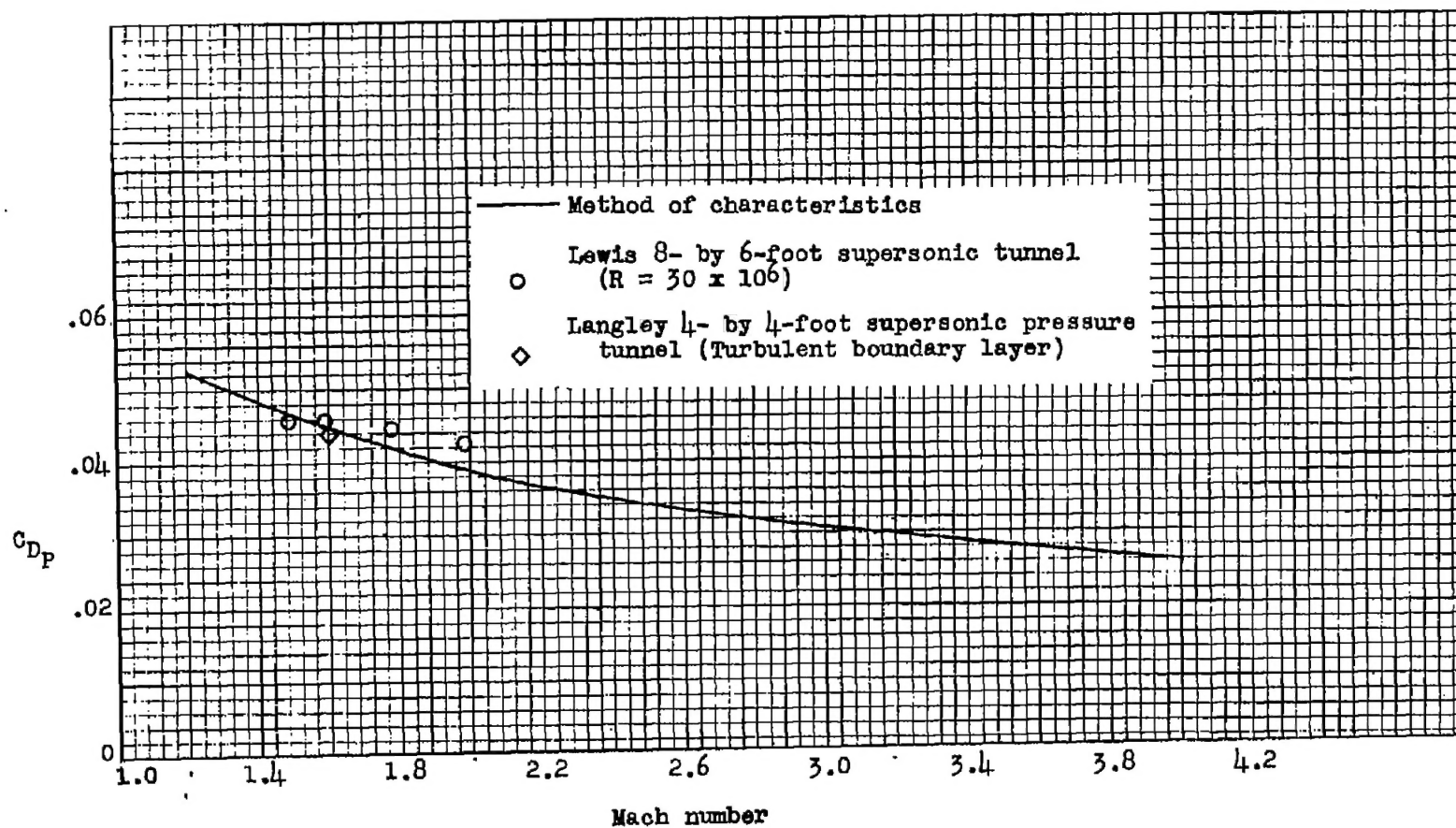


Figure 9.- Estimate of RM-10 forebody pressure drag compared with wind-tunnel measurements.

20

~~CONFIDENTIAL~~

NACA RM L54H09

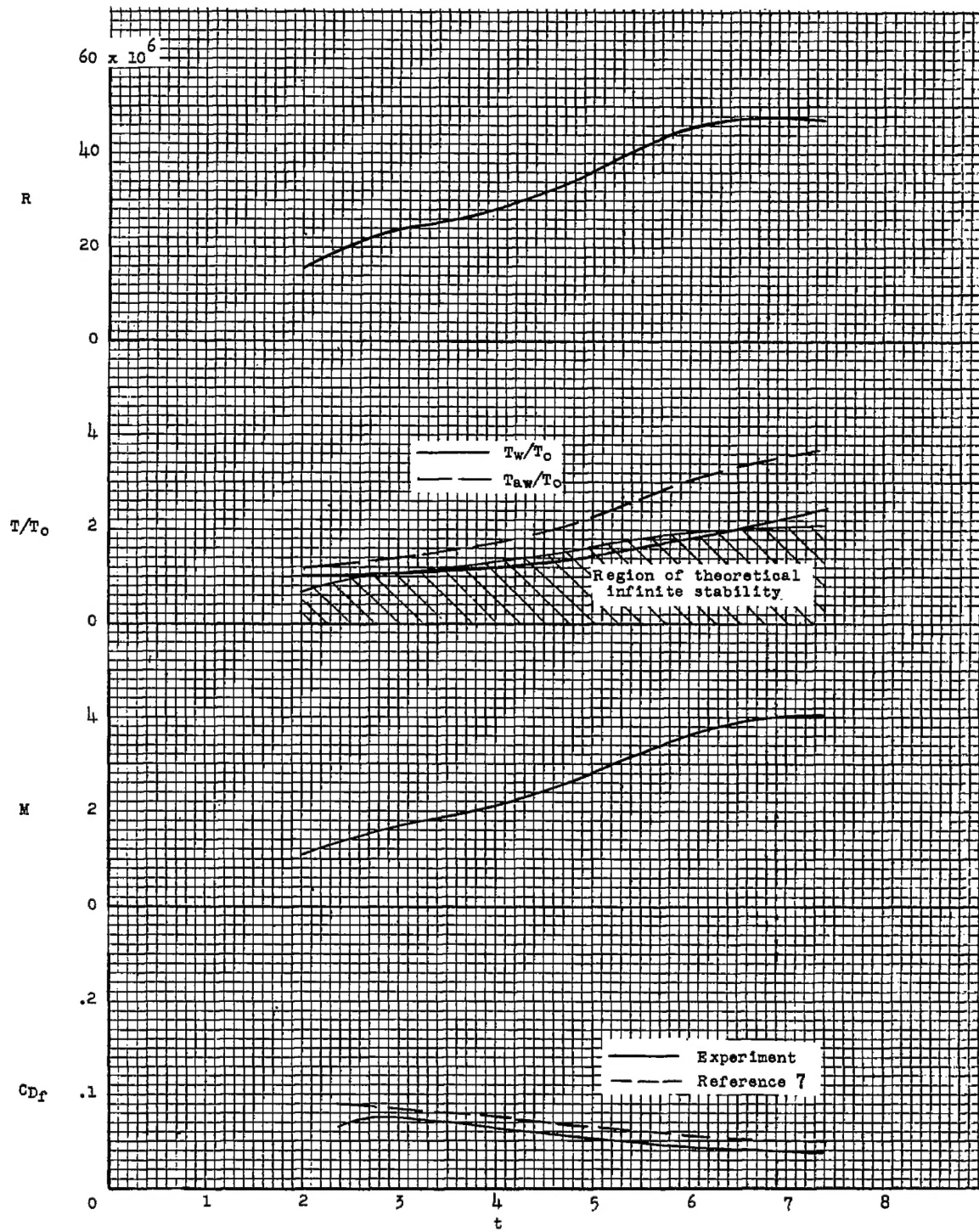


Figure 10.- Variation of friction drag and its affecting parameters with flight time.